




 Cite this: *RSC Adv.*, 2020, 10, 11898

 Received 5th February 2020
 Accepted 18th March 2020

DOI: 10.1039/d0ra01122c

rsc.li/rsc-advances

Flexible and low- k polymer featuring hard–soft-hybrid strategy†

 Huan Hu, Jiajun Ma, * Wen Yuan, Qiuxia Peng and Junxiao Yang *

One of the main challenges for dielectric materials for advanced microelectronics is their high dielectric value and brittleness. In this study, we adopted a hard–soft-hybrid strategy and successfully introduced a hard, soft segment and covalent crosslinked structural unit into a hybridized skeleton via copolymerization of polydimethylsiloxane (PDMS), benzocyclobutene (BCB) and double-decker-shaped polyhedral silsesquioxanes (DDSQ) by a platinum-catalyzed hydrosilylation reaction, thus producing a random copolymer (PDBD) with a hybridized skeleton in the main chain. PDBD exhibited high molecular weight and thermal curing action without any catalyst. More importantly, the cured copolymer displayed high flexibility, high thermal stability and low dielectric constant, evidencing its potential applications in high-performance dielectric materials.

1. Introduction

In recent years, because of the huge public demand, electronic products, especially portable displays and communications and medical devices, have aroused great research interest.^{1,2} Flexible materials that provide mechanical support and electrical interconnection for various functional chips play an important role in the operation of flexible electronic devices. Poly(ethylene terephthalate), poly(dimethylsiloxane) (PDMS), polycarbonate, polyimide, and other polymer materials are commonly used in the electronics industry because of their advantages of ease of use, lightness, and durability.^{3–7} However, the polymers used in electronics are usually thermoplastic resins, which have low thermal stability. To realize the continuous advance of device performance, flexible polymers with low dielectric constant (k) are required to lower the interconnecting resistance/capacity delay, cross-talk, and power dissipation.^{8–10} However, typical polymers in electronics usually have high k (above 3.0), which limits their application in future flexible electronics.^{11,12}

Benzocyclobutene (BCB)-based polymers are new types of thermosetting resins that display physical and chemical properties superior to those of traditional phenolic or epoxy resins because of their unique molecular network formation after thermal curing. Another attractive feature of BCB structure is that they can undergo thermal curing without a catalyst and gaseous by-product formation to yield polybenzocyclobutenes (PBCBs). PBCBs have many excellent properties, including high thermal stability, low water uptake, and favorable k value.^{13–16}

Because of these excellent properties, PBCBs have been widely used as materials for electronics packaging and electrical insulation in the microelectronics industry.^{17,18} A type of BCB-containing resin derived from bis(benzocyclobutenyl) divinyl-tetramethylsiloxane¹⁹ (trade-mark of the DOW Chemical Company) displays a k of 2.65, but it is brittle. Recently, researchers have attempted to improve the properties of PBCBs by incorporating reactive functional units (*e.g.*, adamantyl,²⁰ norbornyl,²¹ silacyclobutyl,²² triazineyl,²³ and double-decker silsesquioxane (DDSQ)²⁴) into BCB monomers. In addition, blending various inorganic compounds (*e.g.*, diamond,²⁵ multiwalled carbon nanotubes,²⁶ or boron nitride nanosheets²⁷) into the BCB resin matrix to form PBCB nanocomposites has also been reported. Nevertheless, these types of PBCBs still display either brittleness or unsatisfactory k after thermal curing, which makes it difficult to meet the requirements of next-generation high-performance dielectrics. Therefore, research on PBCBs with lower k and higher flexibility is of great significance.

Recently, hard–soft hybrid materials combining two more structural units with complementary performance have been reported.^{28–30} The combination of hard and soft units can result in attractive properties that are inaccessible to homogenous materials. Typically, the soft phase offers toughness, whereas the hard phase provides strength.³¹ Because of their attractive properties, hard–soft hybrid materials are suitable for a variety of functions. The best way to combine soft materials with strong but brittle reinforcement materials to achieve both strength and toughness remains a fascinating topic. This paper presents the synthesis of linear PBCBs (denoted as PDBDs) featuring hard–soft-hybrid strategy. As shown in Fig. 1A, the design strategy of PDBDs was based on the high thermostability and low k of the DDSQ backbone (hard segments), the high performance of BCB-

State Key Laboratory of Environmental-friendly Energy Materials, School of Material Science and Engineering, Southwest University of Science and Technology, Mianyang 621010, P. R. China. E-mail: yangjunxiao@swust.edu.cn; jiajunma@yeah.net

† Electronic supplementary information (ESI) available: Experimental section and other characterization data. See DOI: 10.1039/d0ra01122c



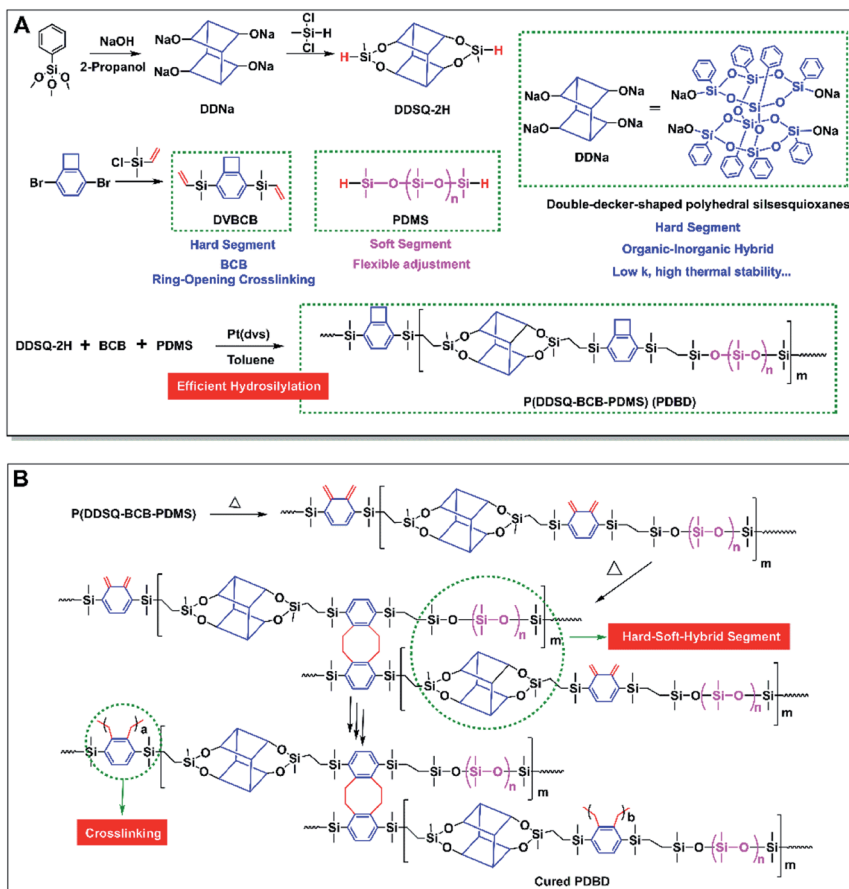


Fig. 1 (A) Synthetic procedure and (B) proposed thermocuring mechanism of PDBDs.

based cross-linked structures (hard segments), and the flexible PDMS units (soft segments).

2. Experimental

Detailed experimental information is included in the ESI†

3. Results and discussion

The PDBDs were efficiently prepared in two steps involving the synthesis of two functional monomers (DDSQ-2H and DVBCB) and their subsequent polymerization by Pt-catalyzed hydrosilylation (see detailed synthesis steps and characterization of chemical structures in ESI†). The high-yield polymerization reaction was conducted in a homogeneous system using toluene as the solvent and Pt(dvs) as the catalyst. Random copolymers with high molecular weight (M_w) of above 30 kg mol^{-1} were obtained (Fig. 2A).

The obtained hard-soft-hybrid polymers have good solubility and excellent film-forming ability. As the existence of BCB group, PDBDs has the property of thermal curing without any catalyst. The crosslinking process and possible reaction mechanism were shown in Fig. 1B and S2 (see in ESI†). In addition, as depicted in Fig. 2B, there may be two forms of crosslinking reaction: (C1) DDSQ-containing fragment and another DDSQ-

containing fragment form a large ring through the crosslinking of BCB-containing fragment. In this process, DDSQ-containing fragment forms its aggregation area and PDMS gathers in another area. (C2) DDSQ-containing fragment and PDMS fragment form a large ring through the crosslinking. According to the calculation results (See ESI† for detailed simulation), the energy of C1 after optimization was less than that of C2. This means that the stability of C1 is higher than that of C2. However, with the increase of DDSQ content, the aggregation of DDSQ begins to appear, which has found in our previous work.²⁴ In addition, the introduction of PDMS prevented the hard parts from aggregating with each other. The crosslinking structure and thus the different types of units displayed good compatibility, even when the content of DDSQ was very high (PDBD-3). Thermo-curing of DVBCB and PDMS, or DVBCB and DDSQ-2H generate incompatible and turbid solid, as shown in Fig. S3 (see in ESI†), mixture of DDSQ-2H and PDMS form one heterogeneous system. The compatibility of the materials is further proved by XRD data, SEM and TEM (Fig. S4 and S5 in ESI†).

The crosslinking structure of the PDBDs was determined by differential scanning calorimetry (DSC) and Fourier transform infrared (FTIR) spectroscopy. As shown in Fig. 2C, the PDBDs showed similar curing temperatures with an onset at $180 \text{ }^\circ\text{C}$ and a maximum thermal curing exothermic peak at $258 \text{ }^\circ\text{C}$

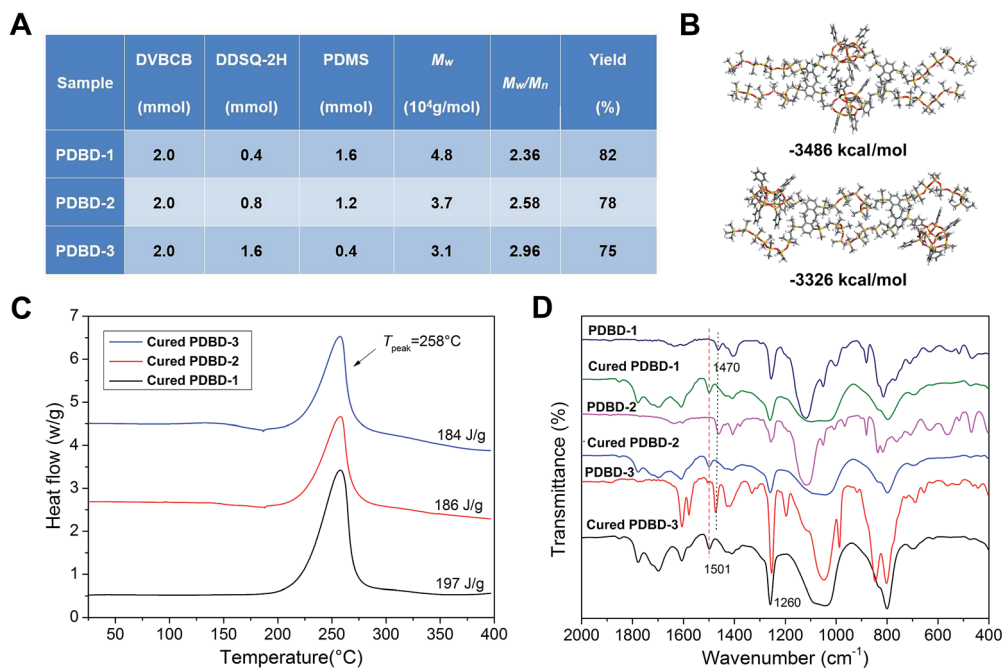


Fig. 2 (A) Synthesis and molecular weight characteristics of PDBDs. (B) Three-dimensional chemical structures of thermocured PDBD with two forms of crosslinking reaction. (C) DSC traces of PDBDs at a heating rate of $10\text{ }^\circ\text{C min}^{-1}$ in N_2 . (D) FTIR spectra of PDBDs before and after thermocuring at $250\text{ }^\circ\text{C}$ for 2 h.

with a reaction heat of $184\text{--}197\text{ J g}^{-1}$.²⁴ Because of its broad range of curing temperature, the PDBDs exhibited good thermal processability. No obvious exothermic peak was observed after the thermocuring reaction of the PDBDs at $250\text{ }^\circ\text{C}$ for 2 h (see Fig. S6 in ESI†).

The thermocuring reaction of PDBDs was also evaluated by FTIR spectroscopy (Fig. 2D). The peaks at 1470 cm^{-1} assigned to a characteristic absorption of BCB (the rocking mode of C–H in the cyclobutene ring of the BCB group) disappeared after thermocuring at $250\text{ }^\circ\text{C}$ for 2 h and were replaced by a new peak at 1501 cm^{-1} . The peak at 1501 cm^{-1} is characteristic of the cyclooctyl structure, which was generated from the coupling reaction between BCB units. These results are in good accordance with those reported for other BCB-containing polymers.^{24,32,33} Therefore, BCB had a limited effect on the DDSQ cages during the thermocuring reaction of PDBDs.

The thermocured PDBD films were light yellow, transparent, flexible, and insoluble in common organic solvents. As shown in Fig. 3A, photographs of the thermocured resins are shown in illustration. The cured PDBD films had excellent transparency of about 90% in the visible region. Their transmittance sharply decreased at wavelengths shorter than 400 nm because of the high phenyl group content of the DDSQ cages and BCB bulk structure. The light transmittance of cured PDBD-1 was slightly higher than that of cured PDBD-2 and PDBD-3, indicating that the increase of PDMS content was helpful to improve the transmittance of the thermocured films.

The combination of the rigid DDSQ cage structure and the flexible PDMS segments in the BCB matrix of PDBDs, linked through covalent bonds, ensured high hydrophobicity of the

films. In addition, the result and discussion for the increased hydrophobicity of the film is added to the ESI† (Page 12).

The thermal properties (Fig. 3B) of the cured PDBD resins were excellent because of the bulky and vacant cage-like structure of DDSQ in the main chain. The 5 wt% weight loss temperatures ($T_{d5\%}$) of the cured PDBD-1, PDBD-2, and PDBD-3 were 457 , 455 , and $459\text{ }^\circ\text{C}$, respectively with 57.8%, 60.4%, and 62.9% residue at $800\text{ }^\circ\text{C}$ in an N_2 atmosphere, respectively. The curves reveal that the thermal stability of the cured PDBD resins decreased slightly as the content of PDMS segments increased. The degradation process of the cured PDBD resins involved two steps: the degradation of the active alkyl chain and the subsequent degradation of the framework, such as aromatic rings and DDSQ cages. Because of the formation of silica from DDSQ moieties and PDMS segments during thermal decomposition, the cured PDBD resins showed high residue contents after degradation. The high thermostability of the cured PDBD resins was attributed to the crosslinked structure of BCB and inorganic DDSQ cages, which enabled it to endure high-temperature processing conditions.

We performed tensile testing to study the mechanical properties of cured PDBD resins. As shown in Fig. 3C, the tensile strength and breaking elongation of the cured PDBD resins were approximately $17.8\text{--}32.1\text{ MPa}$ and $15.6\text{--}31.2\%$, respectively. The excellent flexibility of these PBCBs was mainly caused by the incorporation of PDMS segments. The bulky and vacant DDSQ cages in the main chains substantially enhanced the rigidity of the hybrid materials, restricting the motion of polymer chains. These results illustrate that we can control the mechanical properties of cured PDBD resins by adjusting the

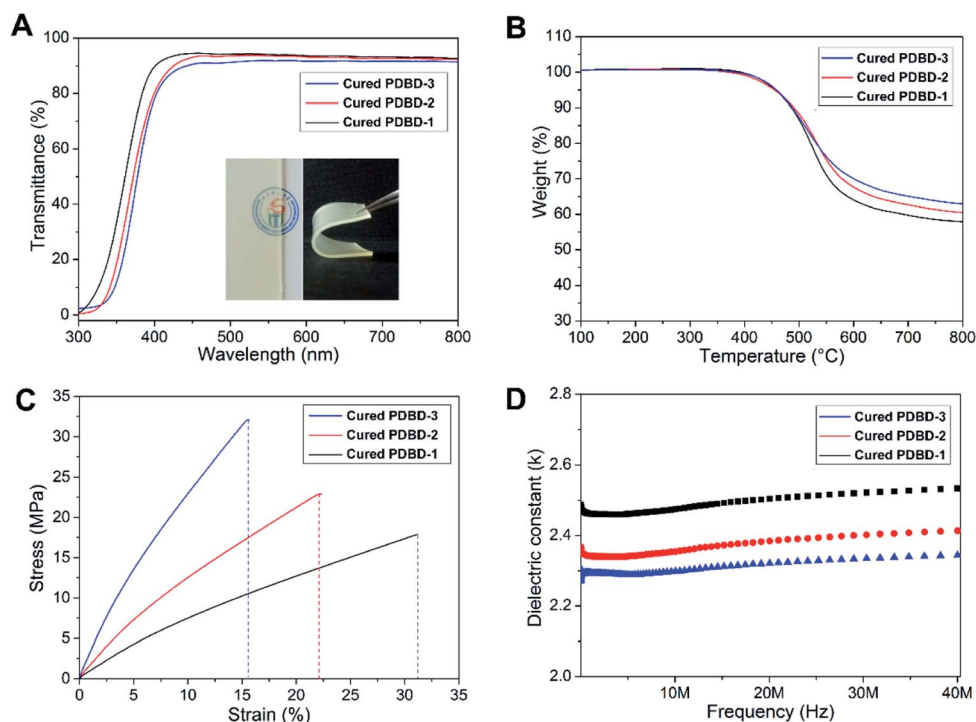


Fig. 3 (A) Transmittance spectra, (B) TGA curves, (C) stress/strain curves, and (D) dielectric properties of the cured PDBD resins. Inset in (B) are photographs of a cured PDBD resin.

Table 1 Important properties of the cured PDBD resins and other resins

Sample	$T_{d5\%}, N_2$	$CY_{800} \text{ } ^\circ\text{C}, N_2$	Tensile strength	Breaking elongation (%)	k
Cured PDBD-1	457 °C	57.8%	17.8 MPa	31.2%	2.51@20 MHz
Cured PDBD-2	455 °C	60.4%	22.9 MPa	22.3%	2.38@20 MHz
Cured PDBD-3	459 °C	62.9%	32.1 MPa	15.6%	2.31@20 MHz
PIM-1 (ref. 34)	—	—	8.1 MPa	9.7%	1.60@10 kHz
sPIM-1/CPTES ³⁴	—	—	29.0 MPa	6.7%	1.67@10 kHz
HMWPSSQ ³⁵	436 °C	84.7%	18.1 MPa	2.6%	2.45@10 MHz
SA9000/epoxy ³⁶	412 °C	25%	62.1 MPa	6.16%	2.91@1 GHz
Porous PI ³⁷	—	—	9–38 MPa	—	1.57–2.40@20 GHz
PEN foam ³⁸	510 °C	—	5.5–11.9 MPa	21.9–59.0%	1.25–1.81@1 kHz

ratio of DDSQ cages to flexible PDMS segments. Detailed mechanical properties of the cured PDBD resins are listed in Table 1.

The k values of the cured PDBD resins were measured by the standard capacity method, and the results are illustrated in Fig. 3D. The k value of each cured resin varied very little with frequency, indicating that they have a stable k in the range of 0–40 MHz. The cured PDBD resins showed k of 2.31–2.51 at 20 MHz, which can be attributed to their relative increase of free volume induced by the DDSQ cages. The cured PDBD-3 exhibited the k of the copolymers of 2.31 at 20 MHz, which was explained by its high DDSQ content. The bulky and vacant cage-like Si–O–Si structures of DDSQ macromers increased the free volume of the copolymer, preventing the polymer chains from packing densely. However, as the DDSQ content increased to a certain amount, the k value of the corresponding cured resin decreased slightly. The

favorable dielectric properties of the cured PDBD resins can be explained by (1) the presence of Si–O–Si and Si–C bonds, which have low polarity, making it difficult to polarize the polymers; (2) the introduction of the bulky and vacant cage-like structure of DDSQ and the BCB cross-linking unit make the related polymer chains unable to reverse chain entanglements. In addition, the cured PDBD resins had hydrophobic surface and low water absorption, as shown in Fig. S7 and S8 in ESI,[†] which effectively prevented moisture adsorption and deterioration of the dielectric properties, and this performance is important for the application of dielectric materials in the microelectronic and electrical industry.

4. Conclusions

We used the hard–soft–hybrid strategy to synthesize random copolymers with a hybridized main chain. The directly

thermocrosslinkable PDBDs were synthesized *via* copolymerization of PDMS, BCB, and DDSQ by Pt-catalyzed hydrosilylation. The resulting random copolymers were converted into cross-linked polymers by the ring-opening reaction of the four-membered ring structure of BCB above 200 °C. The resulting cured resins possessed easy processability, high thermal stability, excellent electrical properties and flexibility, compared with the performance of other BCB-containing resins. As a result, these random copolymers overcame two of the major drawbacks of other PBCBs: brittleness and poor dielectric properties.

Conflicts of interest

There are no conflicts to declare.

Acknowledgements

This work was financially supported by National Nature Science Foundation of China (No. 51603173) and the Project of State Key Laboratory of Environment-friendly Energy Materials, Southwest University of Science and Technology (No. 17FKSY0102 and 18FKSY0206). We thank the China Academy of Physics Engineering for their support of computer simulation.

Notes and references

- 1 Z. Liu, J. Xu, D. Chen and G. Shen, *Chem. Soc. Rev.*, 2015, **44**, 161–192.
- 2 J. Lee, H. Kwon, J. Seo, S. Shin, J. H. Koo, C. Pang, S. Son, J. H. Kim, Y. H. Jang, D. E. Kim and T. Lee, *Adv. Mater.*, 2015, **27**, 2433–2439.
- 3 H. Lee, M. Kim, I. Kim and H. Lee, *Adv. Mater.*, 2016, **28**, 4541–4548.
- 4 H. Jang, Y. J. Park, X. Chen, T. Das, M. S. Kim and J. H. Ahn, *Adv. Mater.*, 2016, **28**, 4184–4202.
- 5 X. Wang, H. Tian, M. A. Mohammad, C. Li, C. Wu, Y. Yang and T. L. Ren, *Nat. Commun.*, 2015, **6**, 7767–7769.
- 6 H. G. Im, B. W. An, J. Jin, J. Jang, Y. G. Park, J. U. Park and B. S. Bae, *Nanoscale*, 2016, **8**, 3916–3922.
- 7 T. Q. Trung, S. Ramasundaram, S. W. Hong and N. E. Lee, *Adv. Funct. Mater.*, 2014, **24**, 3438–3445.
- 8 P. A. Kohl, *Annu. Rev. Chem. Biomol. Eng.*, 2011, **2**, 379–401.
- 9 G. Maier, *Prog. Polym. Sci.*, 2001, **26**, 3–65.
- 10 W. Volksen, R. D. Miller and G. Dubois, *Chem. Rev.*, 2009, **110**, 56–110.
- 11 A. Grill, S. M. Gates, T. E. Ryan, S. V. Nguyen and D. Priyadarshini, *Appl. Phys. Rev.*, 2014, **1**, 11306–11317.
- 12 A. L. Moore and L. Shi, *Mater. Today*, 2014, **17**, 163–174.
- 13 A. K. Sadana, R. K. Saini and W. E. Billups, *Chem. Rev.*, 2003, **103**, 1539–1602.
- 14 M. F. Faroni, *Prog. Polym. Sci.*, 1996, **21**, 505–555.
- 15 Y. Cheng, J. Yang, Y. Jin, D. Deng and F. Xiao, *Macromolecules*, 2012, **45**, 4085–4409.
- 16 A. Flores-Gaspar and R. Martin, *Synthesis*, 2013, **45**, 563–580.
- 17 P. E. Ganrou, W. B. Rogers, D. M. Scheck, Y. Ida and K. Ohba, *IEEE Trans. Adv. Packag.*, 1999, **22**, 487–498.
- 18 A. Modafe, N. Ghalichechian, M. Powers, M. Khbeis and R. Ghodssi, *Microelectron. Eng.*, 2005, **82**, 154–167.
- 19 M. E. Mills, P. Townsend, D. Castillo, S. Martin and A. Achen, *Microelectron. Eng.*, 1997, **33**, 327–334.
- 20 L. Kong, Y. Cheng, Y. Jin, Z. Ren, Y. Li and F. Xiao, *J. Mater. Chem. C*, 2015, **3**, 3364–3370.
- 21 H. W. H. Lai, S. Liu and Y. Xia, *J. Polym. Sci., Part A: Polym. Chem.*, 2017, **55**, 3075–3081.
- 22 H. Hu, L. Liu, Z. Li, C. Zhao, Y. Huang, G. Chang and J. Yang, *Polymer*, 2015, **66**, 58–66.
- 23 J. Zhou, J. Wang, Y. Tao, L. Fang and J. Fang, *ACS Sustain. Chem. Eng.*, 2018, **6**, 5620–5626.
- 24 H. Hu, J. Ma, X. Li, Q. Yin, L. Fan, X. Wei, Q. Peng and J. Yang, *Polym. Chem.*, 2019, **10**, 4551–4560.
- 25 A. Gracias, N. Tokranova and J. Castracane, *Phys. Status Solidi A*, 2011, **208**, 684–690.
- 26 G. Sakellariou, H. Ji, J. W. Mays, N. Hadjichristidis and D. Baskaran, *Chem. Mater.*, 2007, **19**, 6370–6372.
- 27 Q. Li, L. Chen, M. R. Gadinski, S. Zhang, G. Zhang, H. U. Li, E. Iagodkine, A. Haque, L. Chen, T. N. Jackson and Q. Wang, *Nature*, 2015, **523**, 576–579.
- 28 L. Zang, D. Chen, Z. Cai, J. Peng and M. Zhu, *Composites, Part B*, 2018, **137**, 217–224.
- 29 M. Amrollahi, G. M. M. Sadeghi and Y. Kashcooli, *Mater. Des.*, 2011, **33**, 3933–3941.
- 30 B. Kim, C. G. Chae, Y. Satoh, T. Isono, M. K. Ahn, C. M. Min, J. H. Hong, C. F. Ramirez, T. Satoh and J. S. Lee, *Macromolecules*, 2018, **51**, 2293–2301.
- 31 R. O. Ritchie, *Nat. Mater.*, 2011, **10**, 817–822.
- 32 E. Harth, H. B. Van, V. Y. Lee, D. S. Germack, C. P. Gonzales, R. D. Miller and C. J. Hawker, *J. Am. Chem. Soc.*, 2002, **124**, 8653–8660.
- 33 S. F. Hahn, S. J. Martin and M. L. Mckelvy, *Macromolecules*, 1992, **25**, 1539–1545.
- 34 B. Liu, K. G. Haw, C. Zhang, G. Yu, J. Li, P. Zhang, S. Li, S. Wu, J. Li and X. Zou, *Microporous Mesoporous Mater.*, 2020, **294**, 109887–109893.
- 35 J. Mo and W. Ma, *Polym. Sci., Ser. B*, 2019, **61**, 1–11.
- 36 C. H. Chen, Z. C. Gu, Y. L. Tsai, R. J. Jeng and C. H. Lin, *Polymer*, 2018, **140**, 225–232.
- 37 K. Kaki, K. Hosokawa, S. Takagi, H. Mabuchi and M. Ohshima, *Macromolecules*, 2013, **46**, 2275–2281.
- 38 L. Wang, X. Liu, C. Liu, X. Zhou, C. Liu, M. Cheng, R. Wei and X. Liu, *Chem. Eng. J.*, 2020, **384**, 123231.